JAERI-M
87-014

NUMERICAL ANALYSIS OF SAWTOOTH OSCILLATIONS IN JOULE HEATING PLASMA IN JT-60

February 1987

Hiroshi SHIRAI, Keisuke NAGASHIMA, Takeo NISHITANI
and JT-60 Team

日本原子力研究所
Japan Atomic Energy Research Institute

JAERI-Mレポートは，日本原子力研究所が不定期に公刊している研究報告書です。
入手の問合わせは，日本原子力研究所技術情報部情報資料課（〒319-11 茨城県那珂郡東海村）あて，お申しこしください。なお，このほかに財団法人原子力弘済会資料センター（〒319-11 茨城県那珂郡東海村日本原子力研究所内）で複写による実費領布をおこなっております。

JAERI-M reports are issued irregularly.
Inquiries about availability of the reports should be addressed to Information Division Department of Technical Information, Japan Atomic Energy Research Institute, Tokaimura, Naka-gun, Ibaraki-ken 319-11, Japan.

編集兼発行　日本原子力研究所
印　　刷　日青工業株式会社

JAERI-M 87-014

Numerical Analysis of Sawtooth Oscillations in Joule Heating Plasma in JT-60

Hiroshi SHIRAI, Keisuke NAGASHIMA, Takeo NISHITANI
and JT-60 Team

Department of Large Tokamak Research
Naka Fusion Research Establishment
Japan Atomic Energy Research Institute
Naka-machi, Naka-gun, Ibaraki-ken

(Received January 27, 1987)

Characteristics of sawtooth oscillations in soft X ray intensity emitted from JT-60 plasma in Joule heating phase have been numerically studied by using 1-D Tokamak transport code with the model of helical magnetic flux exchange by m=1/n=1 multi-tearing mode. As the plasma current increases, inversion radius of soft X ray intensity and period of sawtooth oscillations increase, and double sawtooth oscillations occur among single sawtooth oscillations.

Occurrence of double sawtooth oscillations is closely related to resistive skin time τ_R. ($= \mu_0 r_1^2/\eta$, where r_1 is inversion radius of soft X ray intensity and η is plasma resistivity) If τ_R becomes larger than critical value τ_R^*, double sawtooth oscillations occur. Results of numerical calculation show that τ_R^* is about 3.0 second, which is in good agreement with the value obtained in experiments.

Keywords: JT-60, Soft X ray, Double Sawtooth Oscillations, Multi-Tearing Mode, Helical Flux Exchange, Inversion Radius, Resistive Skin Time, 1-D Tokamak Transport Code

* T.ABE, H.AIKAWA, N.AKAOKA, H.AKASAKA, M.AKIBA, N.AKINO, T.AKIYAMA, T.ANDO, K.ANNOH, N.AOYAGI, T.ARAI, K.ARAKAWA, M.ARAKI, K.ARIMOTO, M.AZUMI, S.CHIBA, M.DAIRAKU, N.EBISWA, T.FUJII, T. FUKUDA, H.FURUKAWA, K.HAMAMATSU, K.HAYASHI, M.HARA, K.HARAGUCHI, H.HIRATSUKA, T.HIRAYAMA, S.HIROKI, K.HIRUTA, M.HONDA, H.HORIIKE, R.HOSODA, N.HOSOGANE, Y.IIDA, T.IIJIMA, K.IKEDA, Y.IKEDA, T.IMAI, T.INOUE,, N.ISAJI, M.ISAKA, S.ISHIDA, N.ITIGE, T.ITO, Y.ITO, A.KAMINAGA, M.KAWAI, Y.KAWAMATA, K.KAWASAKI, K.KIKUCHI, M.KIKUCHI, H.KIMURA, T.KIMURA, H.KISHIMOTO, K.KITAHARA, S.KITAMURA, A.KITSUNEZAKI, K.KIYONO, N.KOBAYASHI, K.KODAMA, Y.KOIDE, T.KOIKE, M.KOMATA, I.KONDO, S.KONOSHIMA, H.KUBO, S.KUNIEDA, S.KURAKATA, K.KURIHARA, M.KURIYAMA, T.KURODA, M.KUSAKA, Y.KUSAMA,, S.MAEHARA, K.MAENO, S.MATSUDA, S.MASE, M.MATSUKAWA, T.MATSUKAWA, M.MATSUOKA, N.MIYA, K.MIYATI, Y.MIYO, K.MIZUHASHI, M.MIZUNO, R.MURAI, Y.MURAKAMI, M.MUTO, M.NAGAMI, A.NAGASHIMA, K.NAGASHIMA, T.NAGASHIMA, S.NAGAYA, H.NAKAMURA, Y.NAKAMURA, M.NEMOTO, Y.NEYATANI, S.NIIKURA, H.NINOMIYA, T.NISHITANI, H.NOMATA, K.OBARA, N.OGIWARA, T.OHGA, Y.OHARA, K.OHASA, H.OHHARA, T.OHSHIMA, M.OHKUBO, K.OHTA, M.OHTA, M.OHTAKA, Y.OHUCHI, A.OIKAWA, H.OKUMURA, Y.OKUMURA, K.OMORI, S.OMORI, Y.OMORI, T.OZEKI, A.SAKASAI, S.SAKATA, M.SATOU, M.SAIGUSA, K.SAKAMOTO, M.SAWAHATA, M.SEIMIYA, M.SEKI, S.SEKI, K.SHIBANUMA, R.SHIMADA, K.SHIMIZU, M.SHIMIZU, Y.SHIMOMURA, S.SHINOZAKI, H.SHIRAI, H.SHIRAKATA, M.SHITOMI, K.SUGANUMA, T.SUGIE, T.SUGIYAMA, H.SUNAOSHI, K.SUZUKI, M.SUZUKI, M.SUZUKI, N.SUZUKI, S.SUZUKI, Y.SUZUKI, M.TAKAHASHI, S.TAKAHASHI, T.TAKAHASHI, H.TAKAHASHI**, M.TAKASAKI, M.TAKATSU, H.TAKEUCHI, A.TAKESHITA, S.TAMURA, S.TANAKA, T.TANAKA, K.TANI, M.TERAKADO, T.TERAKADO, K.TOBITA, T.TOKUTAKE, T.TOTSUKA, N.TOYOSHIMA, H.TSUDA, T.TSUGITA, S.TSUJI, Y.TSUKAHARA, M.TSUNEOKA, K.UEHARA, M.UMEHARA, Y.URAMOTO, H.USAMI, K.USHIGUSA, K.USUI, J.YAGYU, K.YAMADA, M.YAMAMOTO, O.YAMASHITA, Y.YAMASHITA, K.YANO, T.YASUKAWA, K.YOKOKURA, H.YOKOMIZO, K.YOSHIKAWA, M.YOSHIKAWA, H.YOSHIDA, Y.YOSHINARI, R.YOSHINO, I.YONEKAWA, K.WATANABE

JT−60におけるジュール加熱時の鋸歯状振動の数値解析

日本原子力研究所那珂研究所臨界プラズマ研究部
白井　浩・永島　圭介・西谷　健夫
JT−60チーム

（1987年1月27日受理）

ジュール加熱時にJT−60プラズマから輻射される軟X線強度の鋸歯状振動の特性を，一次元トカマク輸送コードとモード数m＝1／n＝1のマルチ・ティアリング・モードによるヘリカル磁束交換のモデルを用いて数値的に調べた。プラズマ電流が増大すると，軟X線強度の反転半径は増大し，また鋸歯状振動の周期も長くなる。更に，一重鋸歯状振動に混じって二重鋸歯状振動が発生するようになる。

二重鋸歯状振動の発生は，抵抗表皮時間$\tau_R(=\mu_0 r_I^2/\eta$, ここでr_Iは軟X線強度の反転半径，ηはプラズマ抵抗）と密接な関係がある。τ_Rが限界値τ_R^Cを越えた場合には，二重鋸歯状振動が発生する。数値計算で得られたτ_R^Cの値は3.0秒であり，実験で得られた値とよく一致する。

那珂研究所：〒311-02　茨城県那珂郡那珂町大字向山801−1

*

相川 裕史、青柳 哲雄、赤岡 伸雄、赤坂 博美、秋野 昇、秋場 真人、秋山 隆、安積 正史、
阿部 哲也、新井 貴、荒川喜代次、荒木 政則、有本 公子、安東 俊郎、安納 勝人、飯島 勉、
飯田 幸生、池田 幸治、池田 佳隆、井坂 正義、伊佐治信明、石田 真一、市毛 尚志、伊藤 孝雄、
伊藤 康浩、井上多加志、今井 剛、上原 和也、宇佐美広次、牛草 健吉、薄井 勝富、梅原 昌敏、
浦本 保幸、海老沢 昇、及川 晃、大麻 和美、大内 豊、大賀 徳道、大久保 実、大島 貴幸、
太田 和也、太田 充、大高 光夫、大原比呂志、大森憲一郎、大森 俊造、大森 栄和、荻原 徳男、
奥村 裕司、奥村 義和、小関 隆久、小原建治郎、小原 祥裕、神永 敦嗣、河合祝己人、川崎 幸三、
川俣 陽一、菊池 勝美、菊池 満、岸本 浩、北原 勝美、北村 繁、狐崎 晶雄、木村 豊秋、
木村 晴行、清野 公廣、日下 誠、草間 義紀、国枝 俊介、久保 博孝、倉形 悟、栗原 研一、
栗山 正明、黒田 猛、小池 常之、小出 芳彦、児玉 幸三、木島 滋、小林 則幸、小又 将夫、
近藤 育朗、三枝 幹雄、逆井 章、坂田 信也、坂本 慶司、佐藤 正泰、沢畠 正之、郡 守正、
篠崎 信一、柴沼 清、嶋田 隆一、清水 勝宏、清水 正亜、下村 安夫、白井 浩、白形 弘文、
菅沼 和明、杉江 達夫、杉山 隆、鈴木 貞明、鈴木 國弘、鈴木 紀男、鈴木 正信、鈴木 道雄、
鈴木 康夫、砂押 秀則、清宮 宗孝、関 省吾、関 正美、高崎 学、高津 英幸、高橋 春次、
高橋虎之助、高橋 弘法、高橋 実、竹内 浩、竹下 明、田中 茂、田中竹次郎、谷 啓二、
田村 早苗、大楽 正幸、千葉 真一、塚原 美光、次田 友宣、辻 俊二、津田 文男、恒岡まさき、
寺門 恒久、寺門 正之、徳竹 利国、戸塚 俊之、飛田 健次、豊島 昇、中村 博雄、中村 幸治、
長島 章、永島 圭介、永島 孝、永谷 進、永見 正幸、新倉 節夫、西谷 健夫、二宮 博正、
根本 正博、間谷 譲、野亦 英幸、濱松 清隆、林 和夫、原 誠、原口 和三、平塚 一、
平山 俊雄、蛭田 和治、広木 成治、福田 武司、藤井 常幸、古川 弘、細金 延幸、細田隆一郎、
堀池 寛、本田 正男、前野 勝樹、前原 直、間瀬 修次、松岡 守、松川 達哉、松川 誠、
松田慎三郎、水野 誠、水橋 清、宮 直之、宮地 謙吾、三代 康彦、武藤 貢、村井 隆一、
村上 義夫、柳生 純一、安川 亨、矢野 勝久、山下 修、山下 幸彦、山田喜美雄、山本 正弘、
横倉 賢治、横溝 英明 吉川 和仲、吉川 允二、吉田 英俊、吉成 洋治、芳野 隆治、米川 出、
渡辺 和弘、

Contents

目　　次

1. Introduction

Recently new type of sawtooth oscillations in soft X ray intensity have been detected in the experiments of Tokamak devices such as JT-60, TFTR, [1] JET, [2] D-III, [3] and TEXT. [4] In these oscillations, there is another decay in the slow increase phase of soft X ray intensity in one period of sawtooth. This phenomenon is called compound sawtooth oscillation [1] or double sawtooth oscillation. [3]

Several papers about double sawtooth oscillations have been presented. In the paper of Pfeiffer W. et al. [3], 1-D Tokamak simulation and deliberate magnetic flux exchange are combined to reproduce double sawtooth oscillations. In the paper of Denton R. E. et al. [5], Boyd D. A. [6], reduced set of MHD equations have been used to simulate double sawtooth oscillations. The assumption adopted is reduced thermal conductivity coefficients in the plasma center region.

In this paper, we investigate condition for double sawtooth oscillation occurrence. First, consider the mechanism of double sawtooth oscillations. One period of double sawtooth oscillations is made up of two different type of minor disruptions, which means localized not overall sudden energy confinement degradation due to MHD activity. At the first minor disruption, MHD activity is enhanced at region somewhat away from the plasma center. Magnetic flux is locally exchanged and energy stored there is ejected to plasma peripheral region. Plasma center region, however, is left unperturbed. At the second minor disruption, perturbation due to MHD activity extend to plasma center region and energy stored there is ejected to peripheral region. Minor disruption of this type is the same as that of single sawtooth oscillations, which word we use for the sawtooth oscillations observed so far in order to distinguish from double sawtooth oscillations. We call this type of minor disruption internal disruption hereafter.

Distinctive feature of double sawtooth oscillations is the presence of the first minor disruption mentioned above. Such local magnetic flux exchange, due to partial magnetic field reconnection by to m=1 mode, has been numerically calculated. [7] Partial magnetic field reconnection, for short partial reconnection, means magnetic field reconnection which is brought about at the resonant surface and whose region does not extend to plasma center. It occurs when there are two q=1 resonant

surfaces in the plasma and each surface locates close to each other. That is, plasma current profile is hollow. In Joule heated plasma, such profile take places after internal disruption, when temperature profile becomes hollow due to exchange of hot plasma in the plasma center region and cold plasma around q=1 surface. Actually, hollow current profile is experimentally observed at the first minor disruption of double sawtooth oscillations. [8]

Hollow current profile relaxes to the center-peaked one in time. Time scale of this transition is related to resistive skin time τ_R in the plasma center region. In a small Tokamak, value of τ_R is small. Therefore fast magnetic field diffusion leads to existence of only one q=1 resonant surface in the plasma resulting in single sawtooth oscillations occurrence. In a large Tokamak, however, τ_R is large and hollow current profile is kept for long time. In this configuration, local magnetic flux exchange is likely to occur and double sawtooth oscillations appear.

We suppose that there is a critical value in τ_R and when τ_R becomes larger than that, double sawtooth oscillation occur. In order to make sure this, numerical calculation of Joule heated JT-60 plasma has been made by using 1-D Tokamak transport code and model of helical magnetic flux exchange at the minor disruption.

In sec. 2, characteristics of single sawtooth oscillations and double sawtooth oscillations in JT-60 in Joule heating phase are shown. Critical value τ_R^* obtained experimentally is also indicated. In sec. 3, helical magnetic flux exchange by m=1/n=1 multi-tearing are shown and the relation of resistive skin time and double sawtooth oscillations occurrence are mentioned. In sec. 4, model of numerical calculation and results are shown. τ_R^* obtained numerically is also indicated and is compared with experimental value. In sec. 5, results obtained in this paper is summarized.

2. Experimental Results

In JT-60, there are 30 points to install pin diodes to detect soft X ray. 15 pin diodes are fixed every other point at regular interval until shot No. 1566, whose viewing field is shown in Fig. 1 . (Broken line indicates separatrix magnetic surface of shot No. 1089 .) Spatial resolution of detector is about 7 cm. After shot No. 1566, interval of viewing field between ch 7 and ch 8, ch 8 and ch 9, ch 14 and ch 15 becomes 3.5 cm, 10.5 cm, and 3.5 cm respectively. Soft X ray data are sampled every 20 micro second.

Sawtooth oscillations begin 2.5 ~ 3.5 sec after breakdown in 1.0 MA Joule heated hydrogen (H) plasma. Time evolution of soft X ray intensity is shown in Fig. 2. Toroidal field is 4.0 T and q_{eff} is about 5.30 . The distance between viewing chords and plasma center is (a) 1.5 cm, (b) 5.5 cm, (c) 8.5 cm, (d) 15.5 cm, (e) 22.5 cm respectively. Sawtooth oscillations are single sawtooth oscillations. Period of sawtooth oscillations is 25 ~ 30 msec and inversion radius of soft X ray is about 10 cm. These values are independent of plasma density.

In 1.5 MA hydrogen plasma, sawtooth oscillations begin 3.0 ~ 4.0 sec after breakdown. Time evolution of soft X ray intensity is shown in Fig. 3 . Toroidal field is 4.5 T and q_{eff} is about 3.99 . The distance between viewing chords and plasma center is (a) 1.5 cm, (b) 5.5 cm, (c) 12.5 cm, (d) 22.5 cm, (e) 29.5 cm, (f) 36.5 cm respectively. Sawtooth oscillations are single ones for the most part and double sawtooth oscillations are rarely observed. Period of single sawtooth oscillations is 30 ~ 60 msec and period of double ones is 70 ~ 80 msec. Inversion radius of soft X ray is 12 ~ 17 cm.

In 2.0 MA hydrogen plasma, sawtooth oscillations begin 3.5 ~ 4.5 sec after breakdown. AT first, sawtooth oscillations are single sawtooth oscillations. 1.0 ~ 1.5 sec after that, double sawtooth oscillations occur among single sawtooth oscillations at random. In this case, period of single sawtooth oscillations is 50 ~ 80 msec and period of double sawtooth oscillations is 70 ~ 140 msec. Inversion radius of soft X ray intensity is 18 ~ 25 cm. Fig. 4 shows one period of double sawtooth oscillations. The distance between viewing chords and plasma center is (a) 0 cm, (b) 7 cm, (c) 14 cm, (d) 21 cm, (e) 28 cm, (f) 35 cm respectively. Toroidal field is 4.5 T and q_{eff} is 2.95 . At the first

minor disruption of double sawtooth oscillations, m=odd mode (maybe m=1 mode), which can be seen from the phase difference of soft X ray intensity detected at the opposite side of the magnetic axis, is enhanced in the region away from the plasma center. Its location in minor radius is about 21 cm and frequency of the mode is about 1 kHz. Energy stored there is ejected to the peripheral region, whereas plasma center region is left unperturbed. (Slight decrease seen in soft X ray intensity in plasma center viewing chord in Fig. 4 is due to the integrated value of soft X ray emitted from whole plasma region.) At the second disruption, energy stored in the plasma center region is ejected to the peripheral region. Characteristics of this disruption are supposed to be the same as the disruption of single sawtooth oscillations.

In 2.0 MA helium plasma, sawtooth oscillations begins just after the plasma current flattop. It is about 0.5 ~ 1.5 sec earlier than hydrogen case. Time evolution of soft X ray intensity is shown in Fig. 5 . The distance between viewing chords and plasma center is (a) 2 cm, (b) 9 cm, (c) 16 cm, (d) 23 cm, (e) 33.5 cm, (f) 37 cm respectively. Toroidal field is 4.5 T and q_{eff} is about 2.99 . Different from the hydrogen case, only single sawtooth oscillations occur. Its period is 35 ~ 60 msec and inversion radius of soft X ray intensity is 18 ~ 22 cm.

The occurrence of single and double sawtooth oscillations are shown in Fig. 6 in various τ_R and q_{eff}^{-1} value. The value of Z_{eff} used in the calculation of τ_R is determined by JT-60 experimental transport analysis system. [9] Data are consist of divertor and limiter shots of hydrogen plasma and divertor shots of helium plasma. Open symbol indicates single sawtooth oscillations. Close symbol indicates double sawtooth oscillations. This figure shows that critical value for double sawtooth oscillation occurrence is 3.4 ~ 4.5 sec.

3. Double Sawtooth Oscillations and Resistive Skin Time

One period of double sawtooth oscillations is made up of two minor disruptions. Now we pay attention to the first minor disruption. At the first disruption, plasma parameters such as electron temperature are locally exchanged in the region away from the plasma center. This is caused by partial magnetic flux exchange at q=1 resonant surface.

Occurrence of partial magnetic flux exchange due to m=1/n=1 multi-tearing mode has already studied by using reduced set of MHD equations. [7] Here, we review brief outline of the results.

Consider magnetic field configuration with more than one q=1 resonant surfaces in the plasma. Time evolution of plasma parameter follows the reduced set of MHD equations as follows,

$$\frac{\partial \psi}{\partial t} = \nabla\phi \times \nabla\psi \cdot \hat{z} + \eta J_z - E_z \tag{1}$$

$$\frac{\partial \phi}{\partial t} = \nabla\phi \times \nabla V \cdot \hat{z} + \nabla\psi \times \nabla J_z \cdot \hat{z} + \nu \nabla_\perp^2 V \tag{2}$$

Cylindrical coordinate (r, θ, z) is adopted and plasma is considered to be low beta. Equation (1) and (2) are Ohm's law and equation of motion respectively. Here, ψ is helical flux function, ϕ is stream function, V is vorticity, J_z is toroidal current, E_z is toroidal electric field, η is resistivity, ν is viscosity, and $\hat{z}$ is unit vector in the toroidal direction. Toroidal current is expressed by ψ as

$$J_z = \nabla_\perp^2 \psi + \frac{2m}{n} \tag{3}$$

Macroscopic plasma flow $\vec{v}$ is expressed as

$$\vec{v} = \nabla\phi \times \hat{z} \tag{4}$$

and

$$V = \nabla_\perp^2 \phi \tag{5}$$

Initial profile of helical flux function ψ_0 and toroidal current J_{z0} is defined by initial safety factor profile as

$$\psi_0(r) = \frac{B_z}{R}\int_0^r \left(\frac{1}{q} - 1\right) r dr \tag{6}$$

$$J_{z0}(r) = \frac{1}{r}\frac{d}{dr}\left(r\frac{d\psi_0}{dr} + \frac{2m}{n}\right) = \frac{1}{r}\frac{d}{dr}\left(\frac{r^2}{q}\right) \tag{7}$$

Small perturbation is added to this initial equilibrium

configuration. We use the eigenfunction of multi-tearing mode corresponding to the maximum eigen value as perturbation.

Time evolution of helical magnetic flux surface and plasma flow pattern in the plasma for different q profile are shown in Fig. 7 and Fig. 8 . In both cases, there are two q=1 resonant surfaces in the plasma. In the figure, the upper half of the circle shows helical flux contour and lower half shows plasma flow pattern. Unit of time is poloidal *Alfvén* time.

In the first case (fig. 7), helical flux function at the initial state is set as

$$\psi_0(r_{s1}) < \psi_0(r_{s2}) < \psi_0(0) \tag{8}$$

where, r_{s1} and r_{s2} are radius of q=1 resonant surfaces normalized by plasma minor radius, which are 0.361 and 0.584 respectively. In this case, Magnetic field reconnection occurs around q=1 resonant surfaces. But plasma center region (in this case $r < 0.15$) is left unperturbed.

In the other case (Fig. 8), initial helical flux function is set as

$$\psi_0(r_{s1}) < \psi_0(0) < \psi_0(r_{s2}) \tag{9}$$

where, $r_{s1} = 0.281$ and $r_{s2} = 0.590$. In this case, magnetic island appears at the outer q=1 surface. It grows and ejects magnetic axis and and finally covers the whole plasma center region. The condition of partial magnetic flux exchange is presented by eq. (8), that is, there are two q=1 resonant surfaces in the plasma and each surface locates close to each other. If two q=1 surfaces locate apart from each other (satisfying eq. (9)) or there are three q=1 resonant surfaces in the plasma, internal disruption occurs and plasma center region suffers perturbation.

In this paper, we do not put stress on the nonlinear evolution of plasma parameter, but pay attention to the helical magnetic flux exchange before and after the minor disruption.

Results of nonlinear simulation of m=1 multi-tearing mode is summarized in Fig. 9 with time transition of safety factor and helical flux function profiles. Just after the internal disruption, hot plasma core is ejected to outside of the q=1 resonant surface and somewhat cold plasma flows into plasma center region, that is, plasma temperature profile becomes hollow. Then plasma current profile also becomes hollow.

As time goes on, profiles transform from (a) through (d) as indicated in Fig. 9 . If magnetic flux exchange is caused by MHD activity at the stage of (b), partial magnetic flux exchange occurs and plasma center region is left unperturbed. On the other hand, if magnetic flux exchange occurs at the stage of (c) or (d), internal disruption occurs and whole plasma center region is perturbed.

In the plasma with small τ_R value, that is, fast magnetic field diffusion, transition from (a) to (d) is very fast resulting in internal disruption at the stage of (c) or (d). In this case, double sawtooth oscillations do not occur. On the other hand, in the plasma with large τ_R value, that is, slow magnetic field diffusion, long stay at the stage of (b) leads to partial magnetic flux exchange resulting in double sawtooth oscillations. This consideration indicates that critical value exists in τ_R and in the plasma with τ_R larger than this critical value, double sawtooth oscillations occur.

4. Results of Tokamak Transport Simulation

Numerical simulation of sawtooth oscillations has been done as follows. Plasma parameters such as n_i, T_e, T_i, B_θ are numerically calculated by 1-D Tokamak transport equations.

$$\frac{\partial n_i}{\partial t} = -\frac{1}{r}\frac{\partial}{\partial r}(r\Gamma) + S \tag{10}$$

$$\frac{3}{2}\frac{\partial}{\partial t}(n_e T_e) = -\frac{1}{r}\frac{\partial}{\partial r}(rQ_e) + \eta J_z^2 - P_{eq} - P_e \tag{11}$$

$$\frac{3}{2}\frac{\partial}{\partial t}(n_i T_i) = -\frac{1}{r}\frac{\partial}{\partial r}(rQ_i) + P_{eq} - P_i \tag{12}$$

$$\frac{\partial B_\theta}{\partial t} = \frac{\partial}{\partial r}\left\{\frac{\eta}{r}\frac{\partial}{\partial r}(rB_\theta)\right\} \tag{13}$$

S is particle source and Γ, Q_e, Q_i is particle flux, electron heat flux and ion heat flux respectively.

$$\Gamma = -D\frac{\partial n_i}{\partial r} - \Gamma^{in} \tag{14}$$

$$Q_e = -n_e\chi_e\frac{\partial T_e}{\partial r} - \frac{3}{2}DT_e\frac{\partial n_e}{\partial r} \tag{15}$$

As time goes on, profiles transform from (a) through (d) as indicated in Fig. 9 . If magnetic flux exchange is caused by MHD activity at the stage of (b), partial magnetic flux exchange occurs and plasma center region is left unperturbed. On the other hand, if magnetic flux exchange occurs at the stage of (c) or (d), internal disruption occurs and whole plasma center region is perturbed.

In the plasma with small τ_R value, that is, fast magnetic field diffusion, transition from (a) to (d) is very fast resulting in internal disruption at the stage of (c) or (d). In this case, double sawtooth oscillations do not occur. On the other hand, in the plasma with large τ_R value, that is, slow magnetic field diffusion, long stay at the stage of (b) leads to partial magnetic flux exchange resulting in double sawtooth oscillations. This consideration indicates that critical value exists in τ_R and in the plasma with τ_R larger than this critical value, double sawtooth oscillations occur.

4. Results of Tokamak Transport Simulation

Numerical simulation of sawtooth oscillations has been done as follows. Plasma parameters such as n_i, T_e, T_i, B_θ are numerically calculated by 1-D Tokamak transport equations.

$$\frac{\partial n_i}{\partial t} = -\frac{1}{r}\frac{\partial}{\partial r}(r\Gamma) + S \tag{10}$$

$$\frac{3}{2}\frac{\partial}{\partial t}(n_e T_e) = -\frac{1}{r}\frac{\partial}{\partial r}(rQ_e) + \eta J_z^2 - P_{eq} - P_e \tag{11}$$

$$\frac{3}{2}\frac{\partial}{\partial t}(n_i T_i) = -\frac{1}{r}\frac{\partial}{\partial r}(rQ_i) + P_{eq} - P_i \tag{12}$$

$$\frac{\partial B_\theta}{\partial t} = \frac{\partial}{\partial r}\left\{\frac{\eta}{r}\frac{\partial}{\partial r}(rB_\theta)\right\} \tag{13}$$

S is particle source and Γ, Q_e, Q_i is particle flux, electron heat flux and ion heat flux respectively.

$$\Gamma = -D\frac{\partial n_i}{\partial r} - \Gamma^{in} \tag{14}$$

$$Q_e = -n_e\chi_e\frac{\partial T_e}{\partial r} - \frac{3}{2}DT_e\frac{\partial n_e}{\partial r} \tag{15}$$

$$Q_i = -n_i\chi_i\frac{\partial T_i}{\partial r} - \frac{3}{2}DT_i\frac{\partial n_i}{\partial r} \tag{16}$$

D, χ_e, χ_i is plasma diffusion coefficient, electron thermal conductivity, ion thermal conductivity respectively. Γ^{in} is particle inward flow. P_{eq} is energy flow from electron to ion. P_e is Bremsstrahlung and ionization loss. P_i is charge exchange loss.

At each q=1 resonant surface, linear growth rate of m=1/n=1 multi-tearing mode γ is calculated and the width of m=1 magnetic islandS W are

$$W = W_0 \exp\int_t \gamma(t')dt' \tag{17}$$

W_0 is very small initial island width. When magnetic islands which grow at the different q=1 resonant surfaces overlap each other or magnetic island corresponding to the innermost q=1 surface covers the whole region of plasma center, helical magnetic flux is forced to be exchanged. At that moment, helical magnetic flux and plasma density are conserved and plasma temperature is adiabatically changed. The whole processes mentioned above are repeated.

Simulation parameters are chosen considering JT-60 operation in Joule heating phase. Plasma major and minor radius are 3.10 m and 0.83 m respectively. Plasma current is set from 1.5 MA to 2.0 MA. Toroidal field is 4.5 T. Electron line average density is about 3.0×10^{19} m^{-3}. Electron thermal conductivity χ_e is $2.5\times10^{19}/n_eq$ m^2sec^{-1}. Ion thermal conductivity χ_i is set 5 times that of Hinton-Hazaltine's neoclassical χ_i. Plasma diffusion coefficient D is $1.0\times10^{19}/n_e$ m^2sec^{-1}. Plasma resistivity is Spitzer's resistivity. Z_{eff} is assumed to be 1.2 and it is spatially constant.

Intensity of soft X ray emission I_{SX} is also calculated. Only Bremsstrahlung is considered as soft X ray source and it is line integrated along the viewing chord of detector with finite width. (In this case, it is 6 cm.)

$$I_{SX} = \int_V P_{brem}\left\{ \exp(-\frac{E_{cut}^L}{T_e}) - \exp(-\frac{E_{cut}^U}{T_e}) \right\} dv \tag{18}$$

P_{brem} is intensity of Bremsstrahlung, which depends on T_e , n_e and Z_{eff} . E_{cut}^L is lower cutoff energy due to the Beryllium filter installed in front of the detector. Two kinds of filter with different thickness are prepared. E_{cut}^L is 1.4 Kev with 25 μm filter and 4.5 Kev with 1000 μm filter. The former is adopted in the calculation. E_{cut}^U is upper cutoff

energy for detector, which is 23.6 kev.

Fig. 10 shows the time evolution of electron temperatures at (a) 0 cm (thin solid line), (b) 10 cm (thick solid line), (c) 20 cm (dotted line) in 1.5 MA plasma. Single sawtooth oscillations with period of about 20 msec occur. Resistive skin time τ_R is about 1.3 sec. Fig. 11 shows the time evolution of soft X ray intensities. The distance between plasma center and viewing chords are (a) 0 cm, (b) 10 cm, (c) 20 cm respectively.

Fig. 12 shows the time evolution of electron temperatures at (a) 0 cm (thin solid line), (b) 10 cm (thick solid line), (c) 20 cm (dotted line), (d) 30 cm (broken line) in 2.0 MA plasma. Double sawtooth oscillations with period of about 50 msec occur. Resistive skin time τ_R is about 4.8 sec.

Fig. 13 shows the time evolution of soft X ray intensities. The distance between plasma center and viewing chords are (a) 0 cm, (b) 10 cm, (c) 20 cm, (d) 30 cm respectively. Slight saturation of soft X ray intensity can be seen at latter half of one sawtooth period, whereas soft X ray observed experimentally does not saturate even in the case of long period sawtooth ($\sim$ 140 msec). Concentration of metal impurity (perhaps titanium or molybdenum in JT-60) in the plasma center region during one sawtooth period is suspected to be one reason for this discrepancy. Such material enhances soft X ray intensity without changing Z_{eff} . Time evolution of impurity peaking parameter c_v during sawtooth period was studied in PBX Tokamak. [10] It was shown that c_v is small just after the internal disruption, but is large just before the internal disruption, which indicates impurity concentration in the plasma center region during sawtooth period. It is regrettable that spatial profile of Z_{eff} cannot be measured in present JT-60 diagnostic system. Therefore this problem is reserved until future measurement.

Similar calculation with plasma current from 1.5 MA to 2.0 MA are made. Transition of resistive skin time, inversion radius of soft X ray intensity and period of sawtooth oscillations are shown in Fig. 14 by the function of plasma current.

The period of sawtooth oscillations obtained in the simulation is about half of that obtained in the experiments. One reason for this is that trigger of minor disruption is determined by growth rate in cylindrical geometry. If we take into account toroidal effect, reduced growth rate will reproduces sawtooth oscillations with longer period.

It is shown that double sawtooth oscillations occur when τ_R is larger than 3.0 sec. This critical value is almost the same even if trigger of minor disruption is deliberately set considering period of sawtooth oscillations in experiment (50 msec for 1.5 MA and 120 msec for 2.0 MA) .

Sawtooth simulation of 2.0 MA helium plasma is also made. Electron line average density is set 4.1×10^{19} m^{-3} . Z_{eff} is set 3.5 by analogy of experimental data. Mixture rate of helium and hydrogen is set 2. In this case, τ_R is 2.85 sec and double sawtooth oscillations do not occur, which is consistent with the critical value mentioned above. This critical value agrees well with the experimental value obtained in sec. 2 .

5. Summary and Discussion

Double sawtooth oscillations have been numerically reproduced by using 1-D Tokamak transport code with the model of helical magnetic flux exchange due to m=1/n=1 multi-tearing mode. Occurrence of double sawtooth oscillations is closely related to resistive skin time τ_R in the plasma center region. When τ_R becomes larger than critical value τ_R^*, double sawtooth oscillations occur. In JT-60, τ_R^* obtained by experimental data is 3.4 $\sim$ 4.5 sec, which agrees well with the calculated value 3.0 sec.

In this paper, Z_{eff} is assumed to be spatially constant. If inward flow of bulk plasma and impurity (especially light impurity such as carbon or oxygen) is different, profile of Z_{eff} is not constant. Supposing Z_{eff} of plasma center is larger than that of plasma edge, increase of plasma current at the plasma center region after the internal disruption is suppressed and double sawtooth oscillation becomes easy to occur, even if average value of Z_{eff} is the same. On the other hand, if Z_{eff} of plasma center is smaller than that of plasma edge, increase of plasma current at the plasma center region after the internal disruption is enhanced and double sawtooth oscillations become less easy to occur.

Furthermore, model of plasma resistivity can affect critical value

It is shown that double sawtooth oscillations occur when τ_R is larger than 3.0 sec. This critical value is almost the same even if trigger of minor disruption is deliberately set considering period of sawtooth oscillations in experiment (50 msec for 1.5 MA and 120 msec for 2.0 MA) .

Sawtooth simulation of 2.0 MA helium plasma is also made. Electron line average density is set 4.1×10^{19} m^{-3} . Z_{eff} is set 3.5 by analogy of experimental data. Mixture rate of helium and hydrogen is set 2. In this case, τ_R is 2.85 sec and double sawtooth oscillations do not occur, which is consistent with the critical value mentioned above. This critical value agrees well with the experimental value obtained in sec. 2 .

5. Summary and Discussion

Double sawtooth oscillations have been numerically reproduced by using 1-D Tokamak transport code with the model of helical magnetic flux exchange due to m=1/n=1 multi-tearing mode. Occurrence of double sawtooth oscillations is closely related to resistive skin time τ_R in the plasma center region. When τ_R becomes larger than critical value τ_R^c, double sawtooth oscillations occur. In JT-60, τ_R^c obtained by experimental data is 3.4 $\sim$ 4.5 sec, which agrees well with the calculated value 3.0 sec.

In this paper, Z_{eff} is assumed to be spatially constant. If inward flow of bulk plasma and impurity (especially light impurity such as carbon or oxygen) is different, profile of Z_{eff} is not constant. Supposing Z_{eff} of plasma center is larger than that of plasma edge, increase of plasma current at the plasma center region after the internal disruption is suppressed and double sawtooth oscillation becomes easy to occur, even if average value of Z_{eff} is the same. On the other hand, if Z_{eff} of plasma center is smaller than that of plasma edge, increase of plasma current at the plasma center region after the internal disruption is enhanced and double sawtooth oscillations become less easy to occur.

Furthermore, model of plasma resistivity can affect critical value

of double sawtooth oscillations occurrence. From experimental analysis of Joule heating plasma in JT-60, plasma parameters are well explained by using Spitzer's resistivity. For that reason, we use Spitzer's resistivity in this paper. In the plasma which supports neoclassical resistivity not Spitzer's resisitivity, plasma current easily increases in the plasma center after internal disruption, which makes double sawtooth oscillations occurrence slightly difficult.

The critical value τ_R^* is supposed to have some dependence on profile of Z_{eff} , model of plasma resistivity and so on. We must consider their effect in detail to examine double sawtooth oscillation of other Tokamaks. This is now under investigation.

Acknowledgements

The authors wish to express appreciation to Drs. Y. Shimomura, M. Azumi, S. Seki and T. Takizuka and staffs of Large Tokamak Experiment Division for fruitful discussions. The continuous encouragement of Drs. K. Tomabechi, M. Yoshikawa, T. Iijima and Y. Suzuki, is gratefully acknowledged.

References

(1) Yamada H. et al., PPPL-2213 (1985)
(2) Gill R. D. et al., Bull. Am. Phys. Soc., 29, 1305 (1984)
(3) Pfeiffer W., Nucl. Fusion, 25, 673 (1985)
(4) Kim S. B., Nucl. Fusion, 26, 1251 (1986)
(5) Denton R. E., Drake J. F., Kleva R. G., Boyd D. A., Phys. Rev. Lett., 56, 2477 (1986)
(6) Boyd D. A. et al., IAEA-CN-47/A-VI-4 (1986)
(7) Shirai H., Azumi M., JAERI-M 86-024 (1986) (in Japanese)
(8) Taylor G. et al., Nucl. Fusion, 26, 339 (1986)
(9) Shimizu K., Hirayama T., Tani K., Kikuchi M., "Experimental Transport Analysis System in JT-60" in preparation to JAERI-M report
(10) Ida K., Fonck R. J., Hulse R. A., LeBlanc B., PPPL-2264 (1985)
(11) Sillen R. M. J. et al., Nucl. Fusion, 26, 303 (1986)

Acknowledgements

*

The authors wish to express appreciation to Drs. Y. Shimomura, M. Azumi, S. Seki and T. Takizuka and staffs of Large Tokamak Experiment Division for fruitful discussions. The continuous encouragement of Drs. K. Tomabechi, M. Yoshikawa, T. Iijima and Y. Suzuki, is gratefully acknowledged.

References

(1) Yamada H. et al., PPPL-2213 (1985)
(2) Gill R. D. et al., Bull. Am. Phys. Soc., 29, 1305 (1984)
(3) Pfeiffer W., Nucl. Fusion, 25, 673 (1985)
(4) Kim S. B., Nucl. Fusion, 26, 1251 (1986)
(5) Denton R. E., Drake J. F., Kleva R. G., Boyd D. A., Phys. Rev. Lett., 56, 2477 (1986)
(6) Boyd D. A. et al., IAEA-CN-47/A-VI-4 (1986)
(7) Shirai H., Azumi M., JAERI-M 86-024 (1986) (in Japanese)
(8) Taylor G. et al., Nucl. Fusion, 26, 339 (1986)
(9) Shimizu K., Hirayama T., Tani K., Kikuchi M., "Experimental Transport Analysis System in JT-60" in preparation to JAERI-M report
(10) Ida K., Fonck R. J., Hulse R. A., LeBlanc B., PPPL-2264 (1985)
(11) Sillen R. M. J. et al., Nucl. Fusion, 26, 303 (1986)

Appendix Relation between r_I , r_s and r_c

In the experiment, inversion radius of soft X ray intensity r_I and radius of region where sudden change in soft X ray intensity can be seen just after the internal disruption (hereafter, we simply call it "critical radius" and express it by r_c) are obtained. But radius of q=1 resonant surface r_s cannot be found out experimentally because there is only one channel of Faraday rotation detector in JT-60, which does not give us precise information about current profile especially at the plasma center region.

In numerical simulation, on the other hand, r_s and r_c are calculated but r_I cannot be easily obtained because detected soft X ray is consist of many components such as Bremsstrahlung, ray from radiative recombination and so on. In order to calculate intensity of radiative recombination ray, for example, impurity species, its content and spatial profile must be known beforehand. But full information mentioned above is difficult to obtain from experiment.

r_I has been often identified as r_s so far, although the difference between them has been occasionally pointed out. [11] In this section, we examine relation between r_I , r_s and r_c . Electron temperature profile is set as follows.

$$T_e(r) = (1.5\times10^3 - 50)\{ 1.0 - (\frac{r}{a})^l \}^m + 50 \qquad (A\text{-}1)$$

l and m are determined afterward. Electron density is 4.0×10^{19} m^{-3} (const) and Z_{eff} is set 1.2 . Plasma current is assumed to be proportional to $T_e^{3/2}$.

First, safety factor at the plasma surface q(a) is set. If q=1 resonant surface exists in the plasma, helical magnetic flux exchange with redistribution of plasma parameter is forced to be made. From profiles of soft X ray intensity I_{SX} calculated by eq. (18) before and after the helical flux exchange, r_I is obtained.

Calculation has been done for peaked temperature profile (l = 2 , m = 2 in eq. (A-1)) and rounded temperature profile (l = 3 , m = 1) with wide range of q(a). Values of r_c and r_s is obtained by the function of r_I in Fig. 15 for peaked profile. From this figure, relation $r_s/a = 1.35\ r_I/a$ and $r_c/a = 1.96\ r_I/a$ are found out. The same calculation is made for rounded profile , which is shown in Fig. 16 .

From this figure, relation $r_s/a = 1.37\ r_l/a$ and $r_c/a = 1.86\ r_l/a$ are found out. After all, regardless of temperature profile, relation between r_l , r_s and r_c is roughly expressed as

$$r_s \sim 1.4\ r_l \qquad (A\text{-}2)$$

$$r_c \sim 2.0\ r_l \qquad (A\text{-}3)$$

The relation (A-3) is also obtain experimentally. Fig. 17 shows change in soft X ray intensity $\Delta I_{SX}/I_{SX}$ at the different viewing chords at the minor disruption in 2.0 MA plasma. Two positions where $\Delta I_{SX}/I_{SX} = 0$ indicate r_l and r_c . From this figure, relation $r_c = 2\ r_l$ holds.

Refinement of eq. (A-2) and (A-3) in the presence of impurity considering radiative recombination for soft X ray source, or in the case of plasma with slight hollow temperature profile is being calculated now. The results will be presented in another JAERI-M report.

By using eq. (A-2), dependence of r_s/a on q_{eff}^{-1} is calculated, which is shown in Fig. 18 . Open circle indicates JT-60 OH plasma, Close circle indicates JT-60 NBI plasma. Both case include divertor and limiter configuration. For reference, data of DIVA plasma are also shown with open square symbol. In DIVA case, temperature is rather low comparing with JT-60 plasma, the relation, $r_s \sim 1.1\ r_l$, which is obtained with the same calculation, is used. By this figure, relation $r_s/a = q_{eff}^{-1}$ approximately holds.

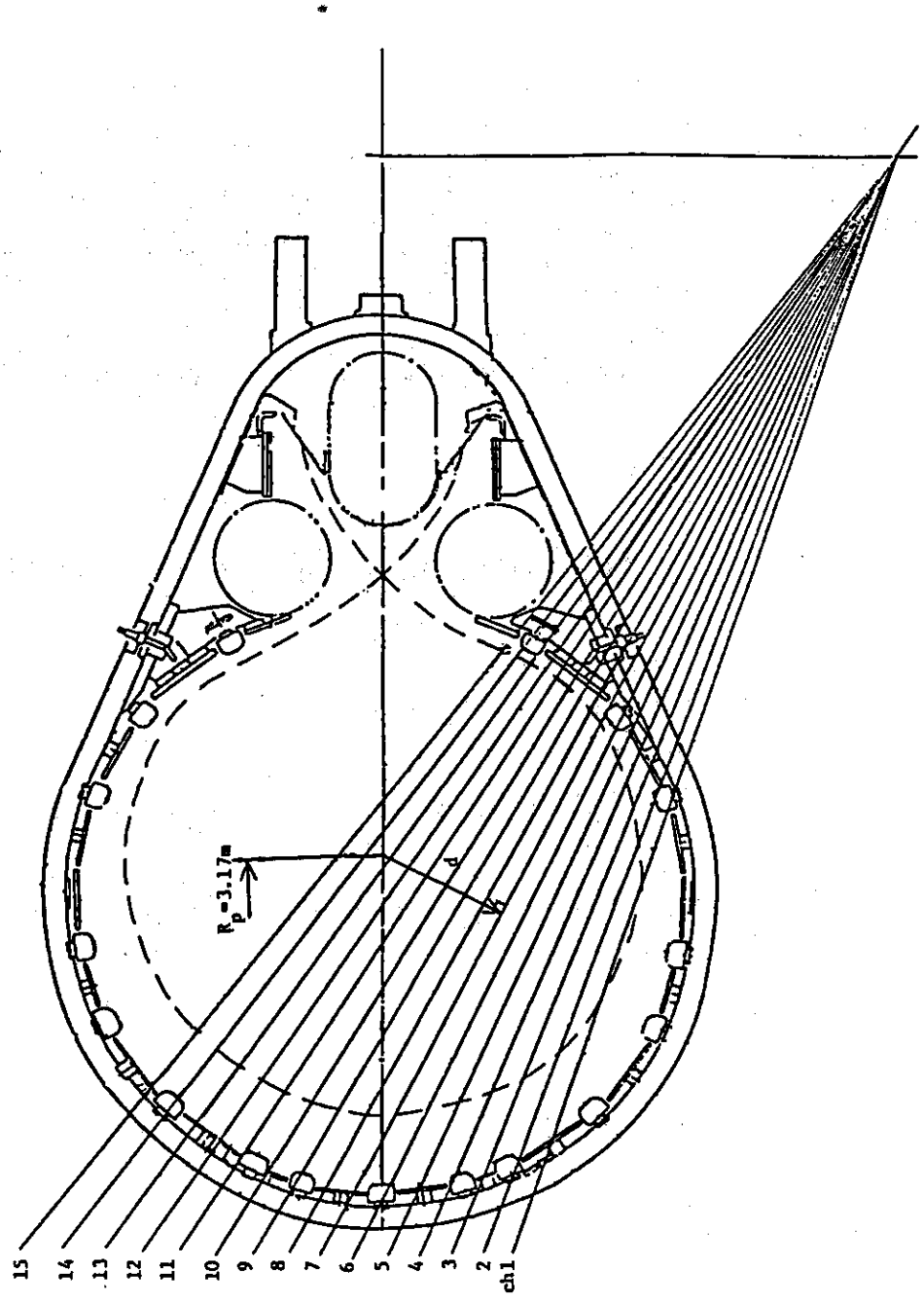

Fig. 1 Poloidal cross section of JT-60 and viewing field geometry of 15 pin diode array. Spatial resolution of detector is about 7 cm. Broken line indicates separatrix magnetic surface.

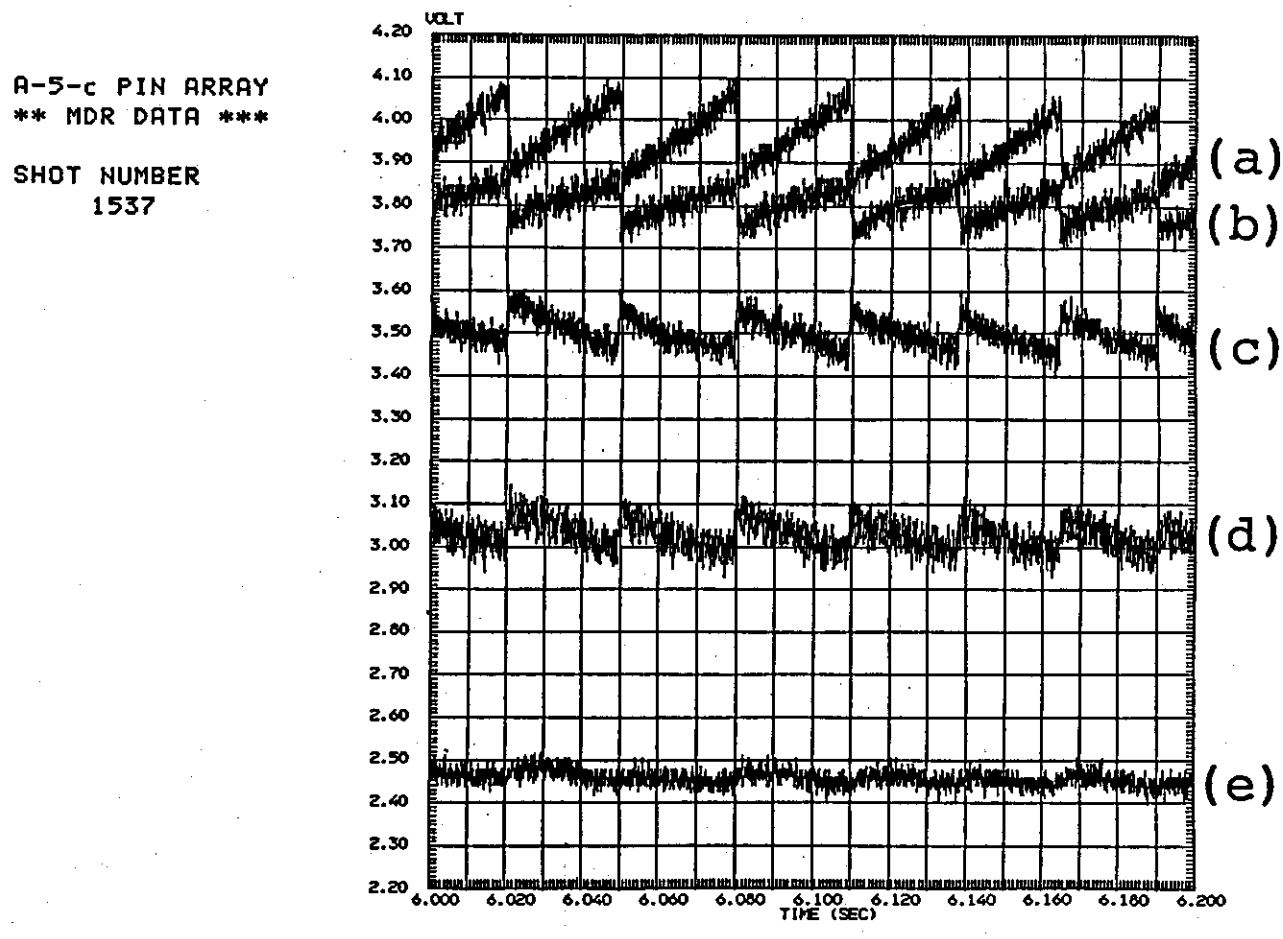

Fig. 2 Time evolution of soft X ray intensity in 1.0 MA hydrogen discharge. (single sawtooth oscillations) The distance between viewing chords and plasma center is (a) 1.5 cm, (b) 5.5 cm, (c) 8.5 cm, (d) 15.5 cm, (e) 22.5 cm respectively.

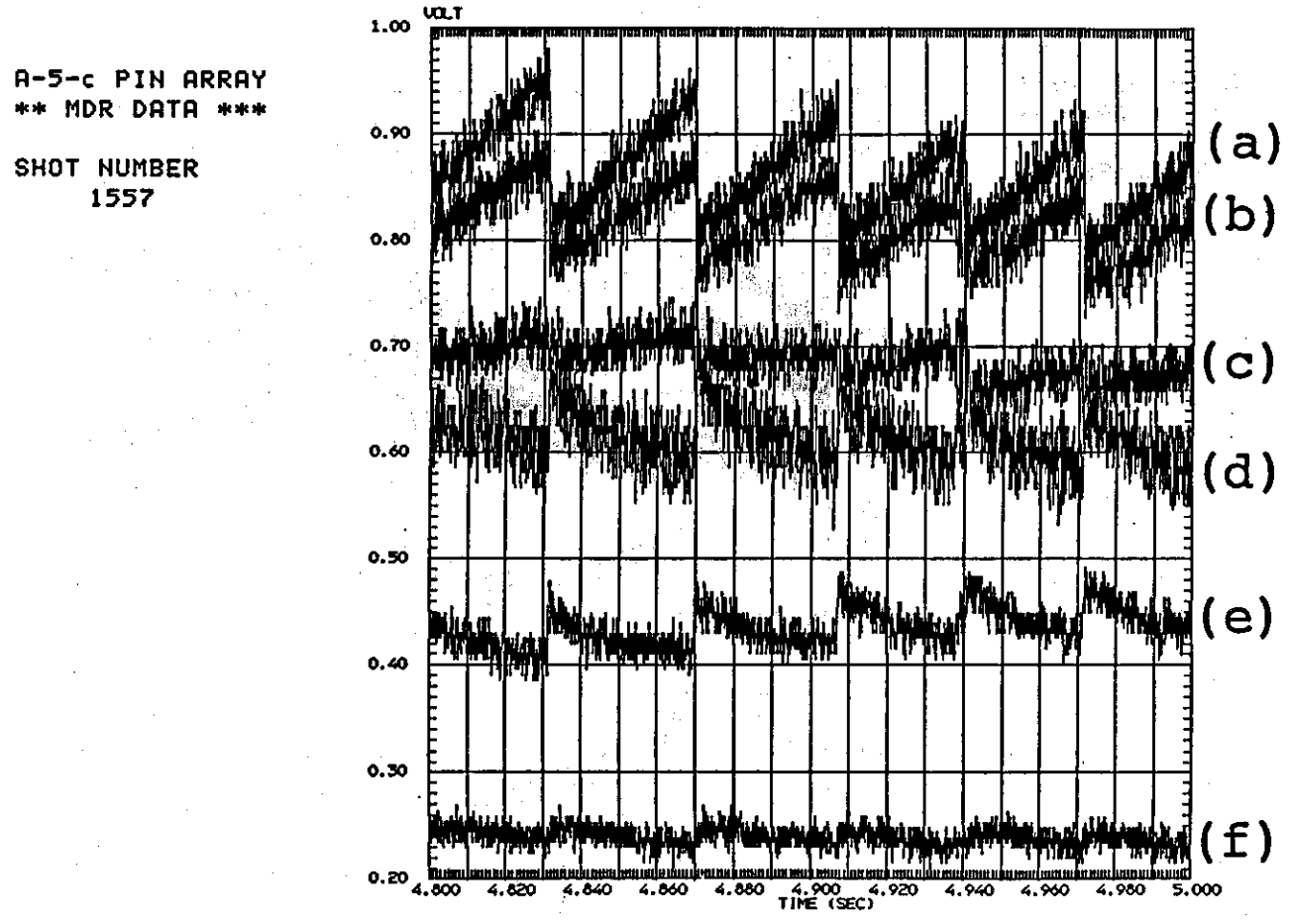

Fig. 3 Time evolution of soft X ray intensity in 1.5 MA hydrogen discharge. (single sawtooth oscillations) The distance between viewing chords and plasma center is (a) 1.5 cm, (b) 5.5 cm, (c) 12.5 cm, (d) 22.5 cm, (e) 29.5 cm, (f) 36.5 cm respectively.

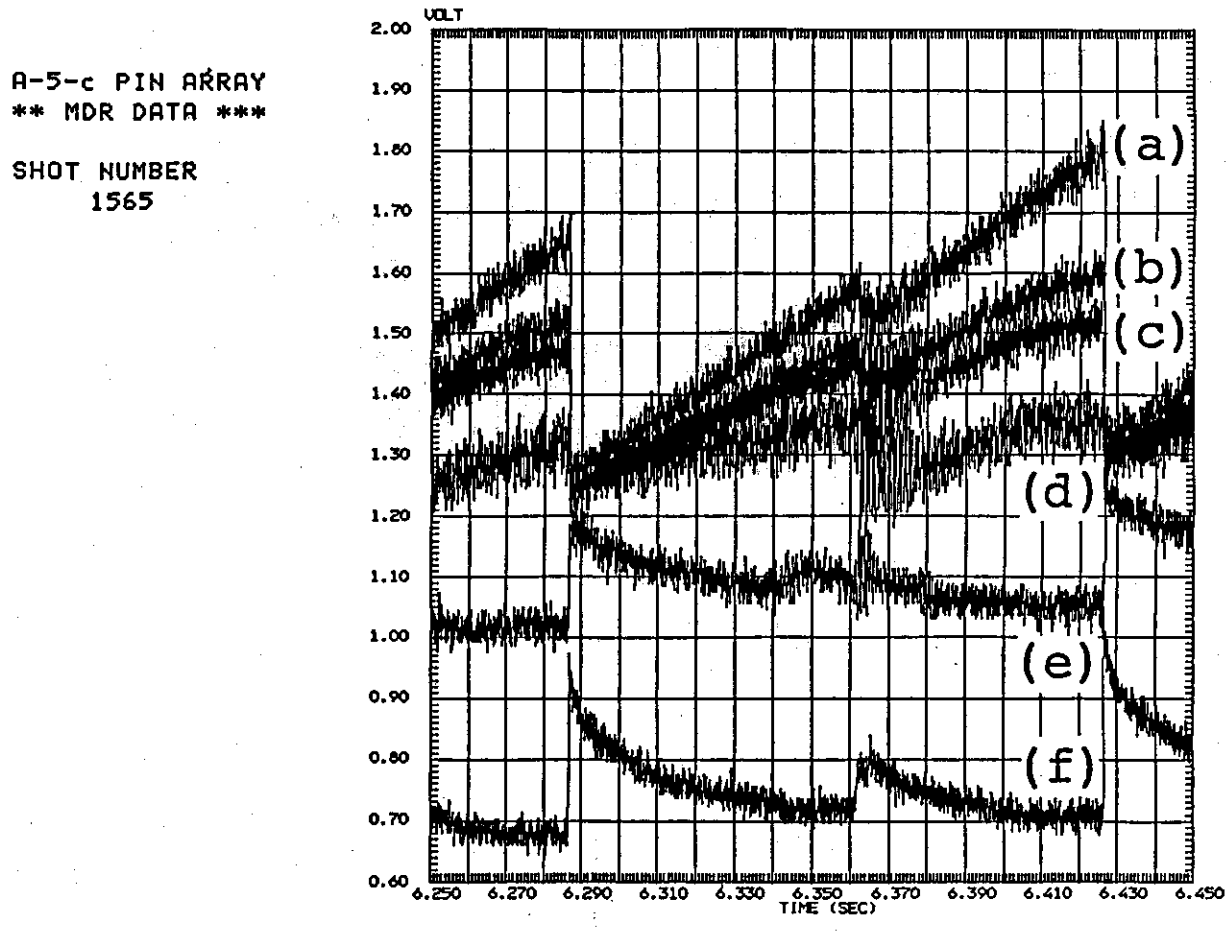

Fig. 4 Time evolution of soft X ray intensity in 2.0 MA hydrogen discharge. (double sawtooth oscillations) The distance between viewing chords and plasma center is (a) 0 cm, (b) 7 cm, (c) 14 cm, (d) 21 cm, (e) 28 cm, (f) 35 cm respectively.

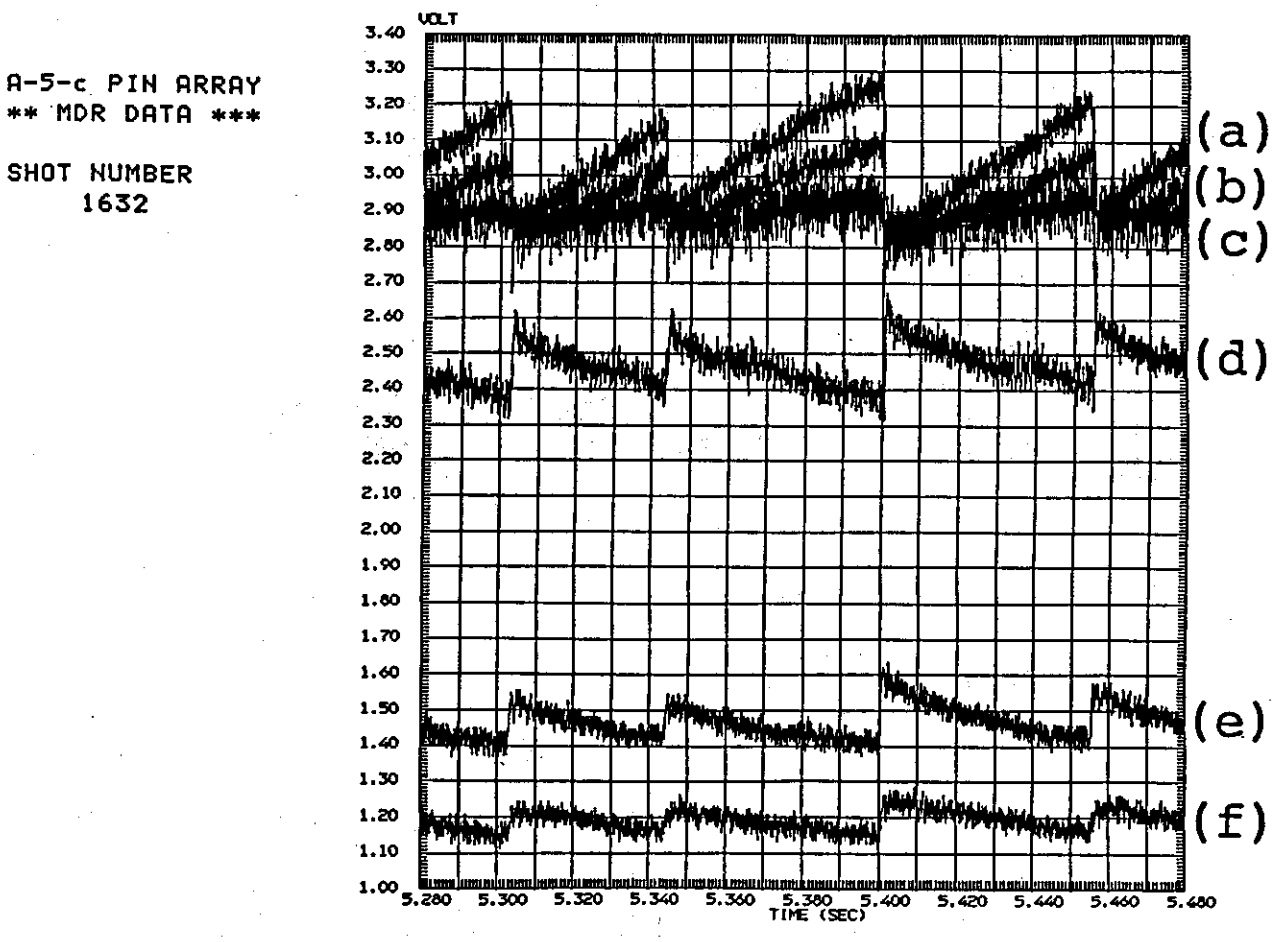

Fig. 5 Time evolution of soft X ray intensity in 2.0 MA helium discharge. (single sawtooth oscillations) The distance between viewing chords and plasma center is (a) 2 cm, (b) 9 cm, (c) 16 cm, (d) 23 cm, (e) 33.5 cm (f) 37 cm respectively.

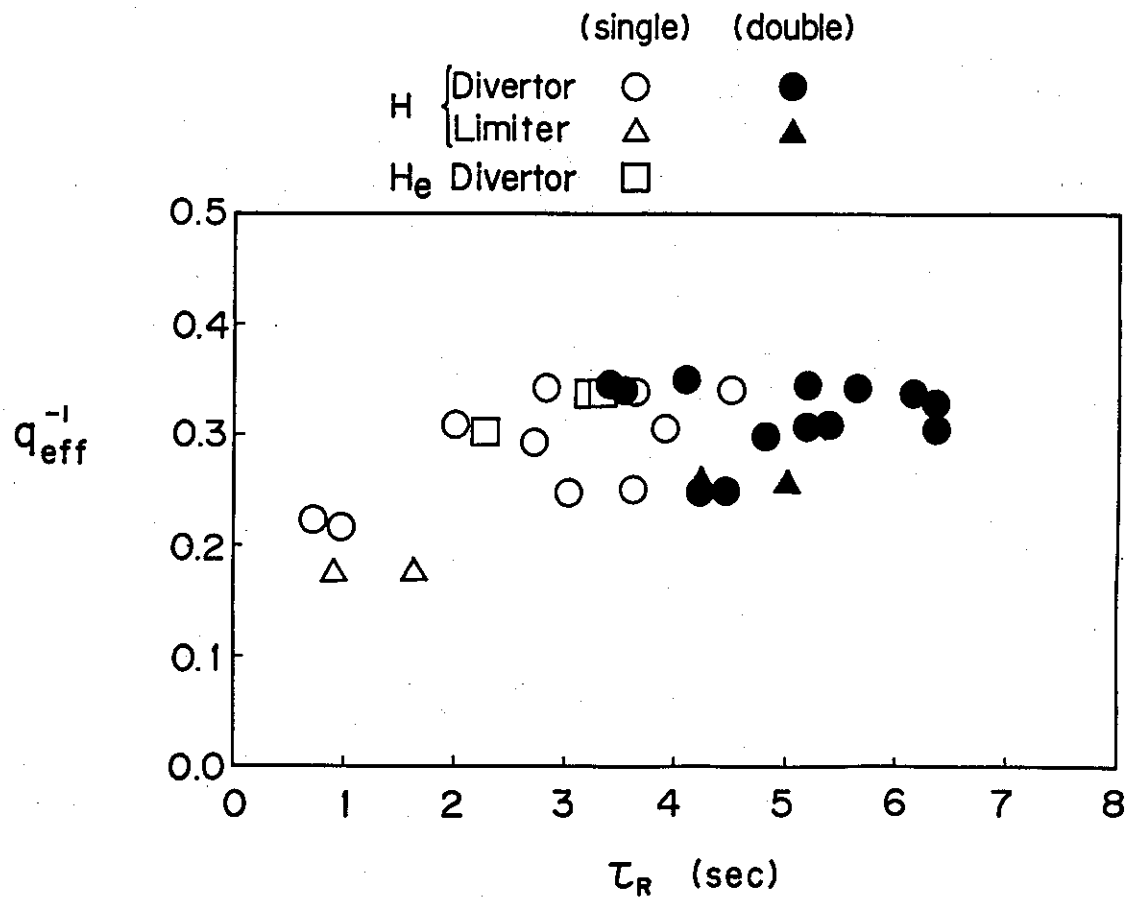

Fig. 6 Classification of single sawtooth oscillations and double sawtooth oscillations in divertor shots of hydrogen plasma (circle), limiter shots of hydrogen plasma (triangle) and divertor shots of helium plasma (square). Open symbol indicates single sawtooth oscillation and close symbol indicates double sawtooth oscillation. Transition from single sawtooth oscillations to double sawtooth oscillations occurs at the value of resistive skin time 3.4 ∿ 4.5 sec.

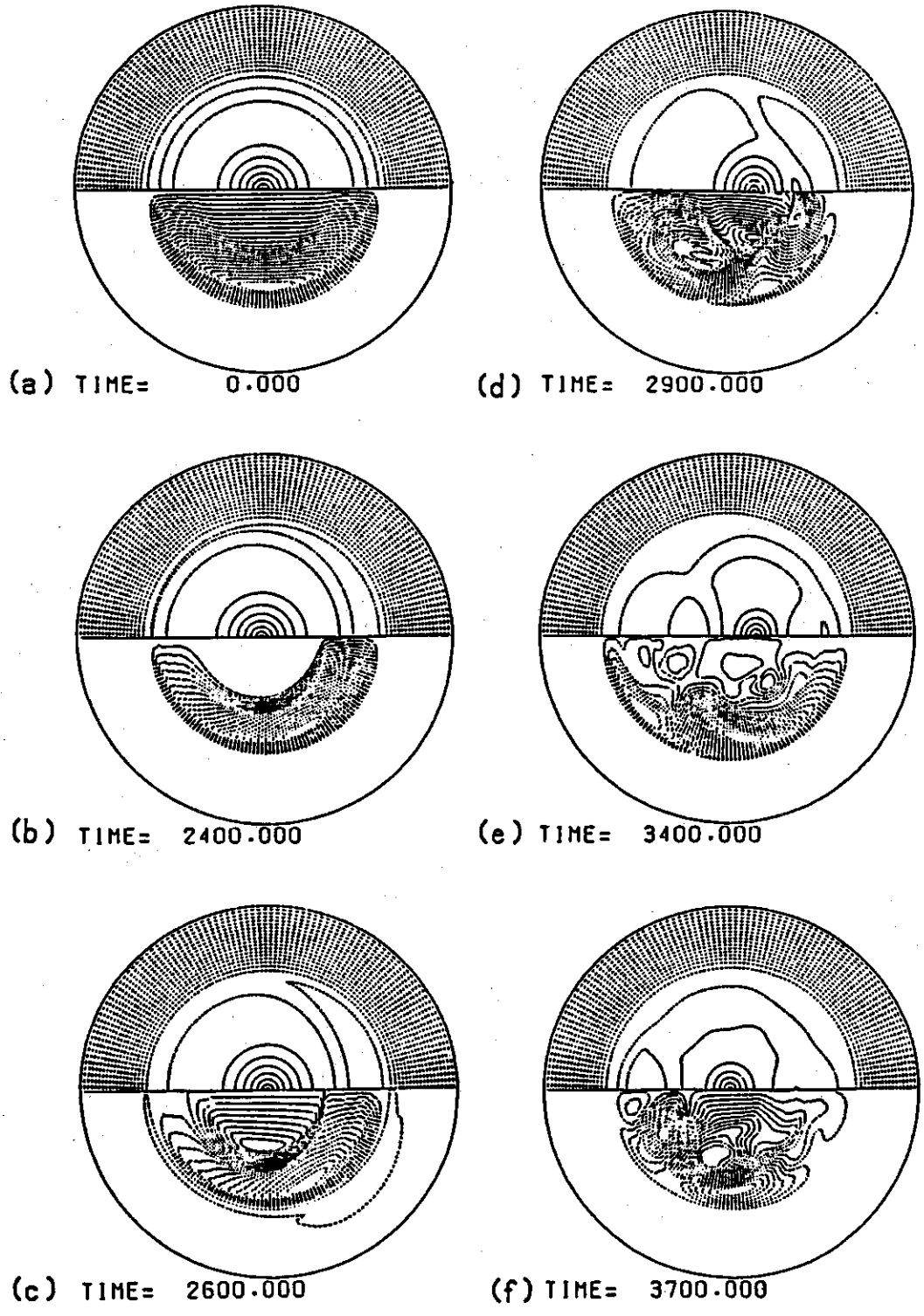

Fig. 7 Time evolution of helical flux surface (upper half of the circle) and plasma flow pattern (lower half) in the case of $\psi_0(r_{s1}) < \psi_0(r_{s2}) < \psi_0(0)$. q = 1 resonant surfaces locate at r_{s1} = 0.361 and r_{s2} = 0.584 respectively. Unit of time is poloidal *Alfvén* time. Partial magnetic flux exchange occurs.

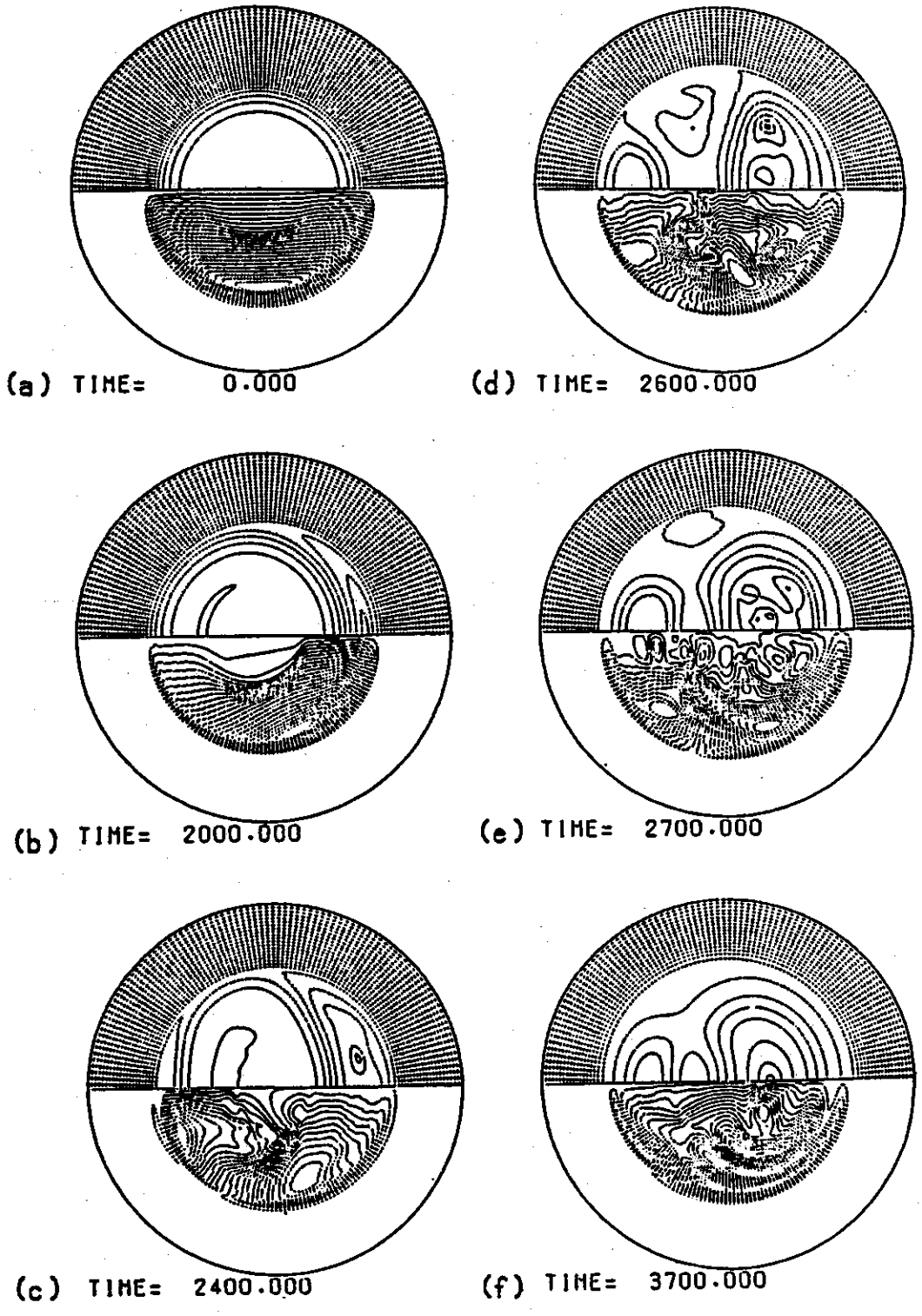

Fig. 8 Time evolution of helical flux surface (upper half of the circle) and plasma flow pattern (lower half) in the case of $\psi_0(r_{s1}) < \psi_0(0) < \psi_0(r_{s2})$. q = 1 resonant surfaces locate at r_{s1} = 0.281 and r_{s2} = 0.590 respectively. Internal disruption occurs.

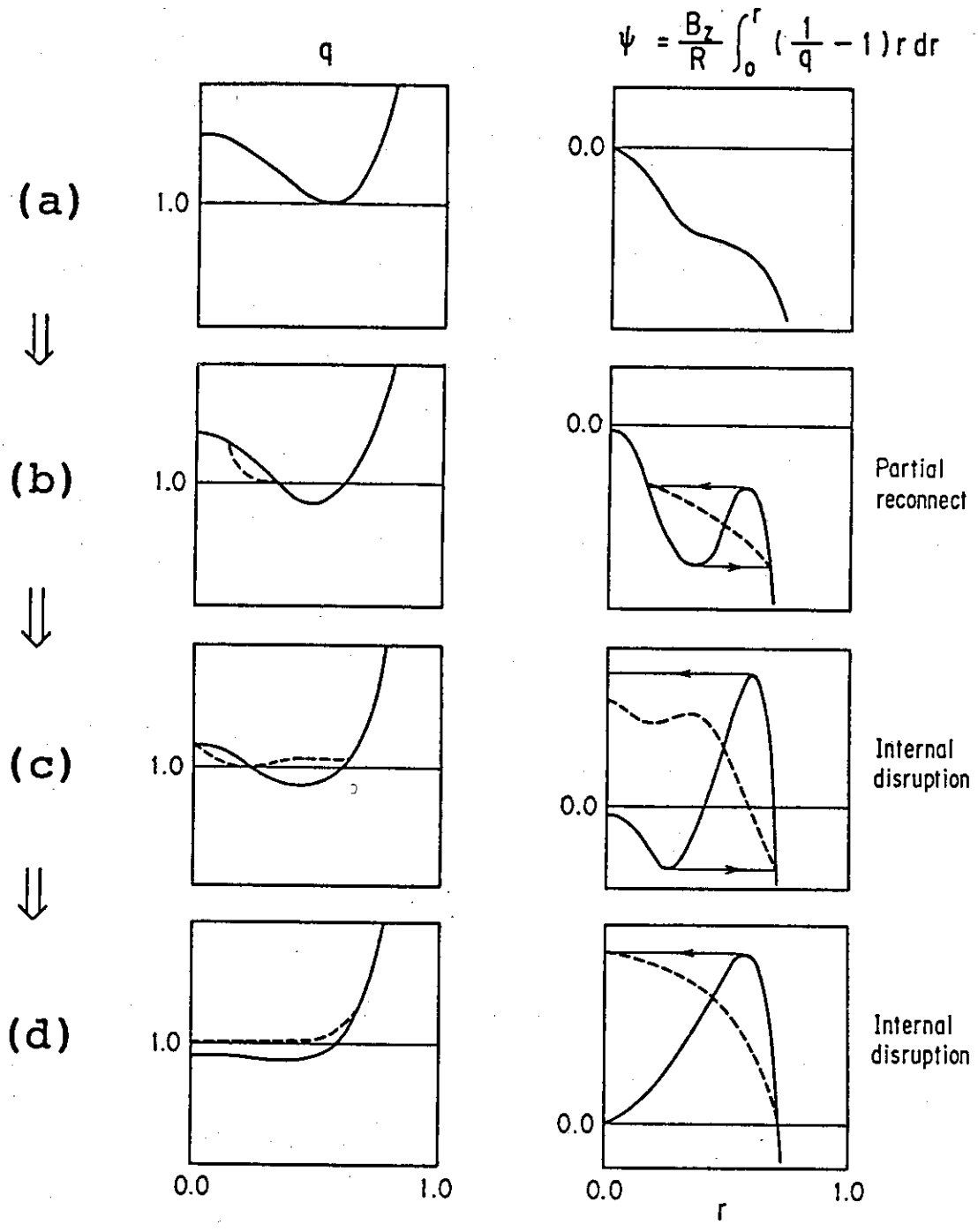

Fig. 9 Time transition of safety factor and helical flux function profiles. If magnetic flux exchange occurs at the stage of (b), it results in partial magnetic flux exchange. If magnetic flux exchange occurs at the stage of (c) or (d), it results in internal disruption.

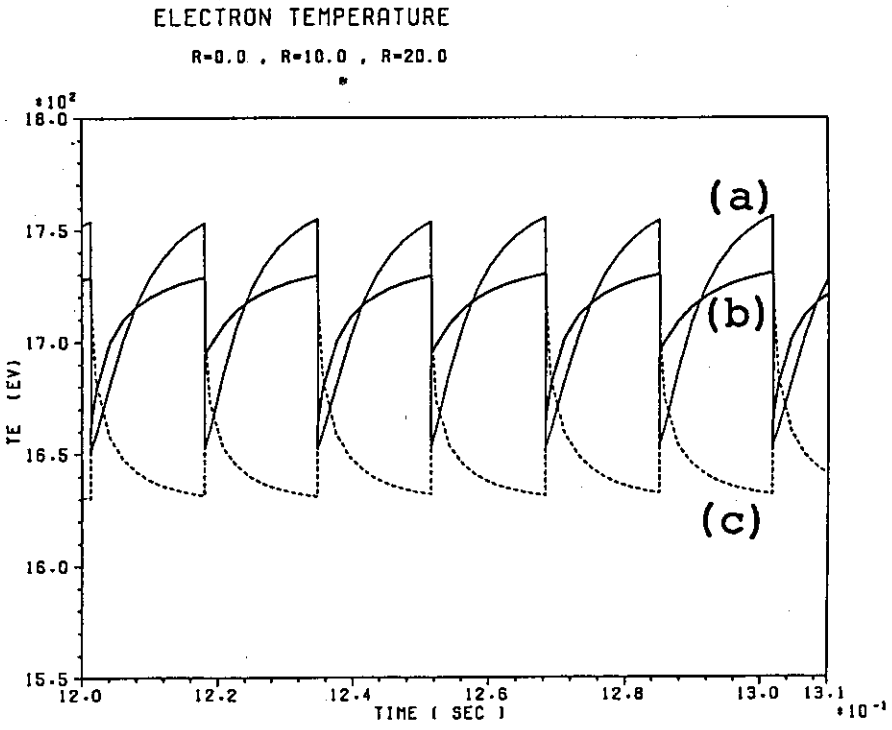

Fig. 10 Time evolution of electron temperature by numerical calculation at (a) r = 0 cm, (b) r = 10 cm, (c) r = 20 cm in 1.5 MA hydrogen plasma. Single sawtooth oscillations with the period of 20 msec are observed.

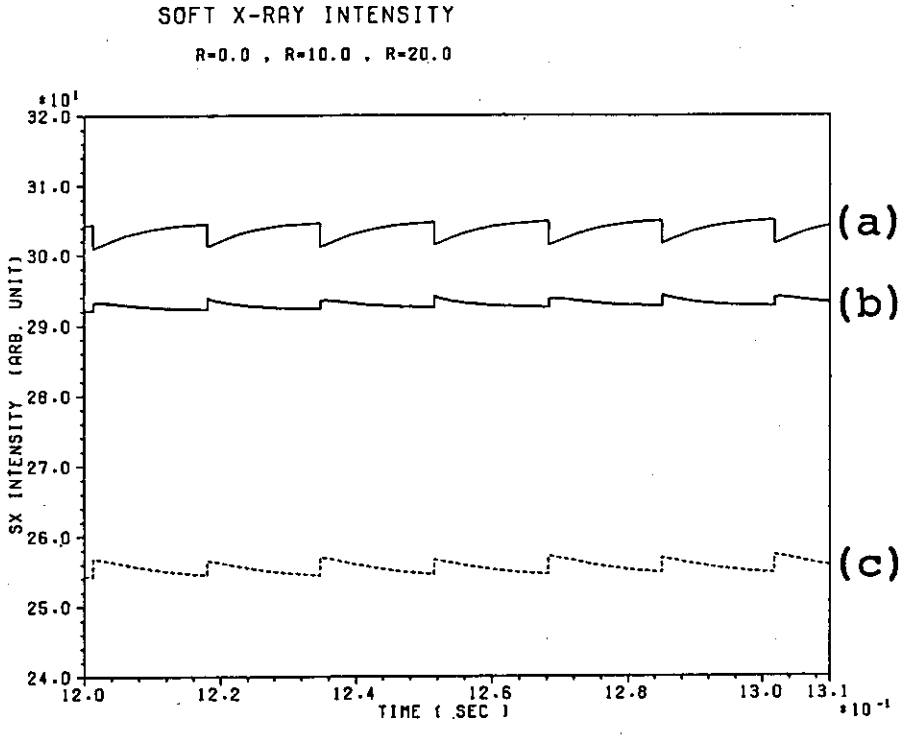

Fig. 11 Time evolution of soft X ray intensity by numerical calculation in 1.5 MA hydrogen plasma. The distance between plasma center and viewing chord is (a) r = 0 cm, (b) r = 10 cm, (c) r = 20 cm respectively.

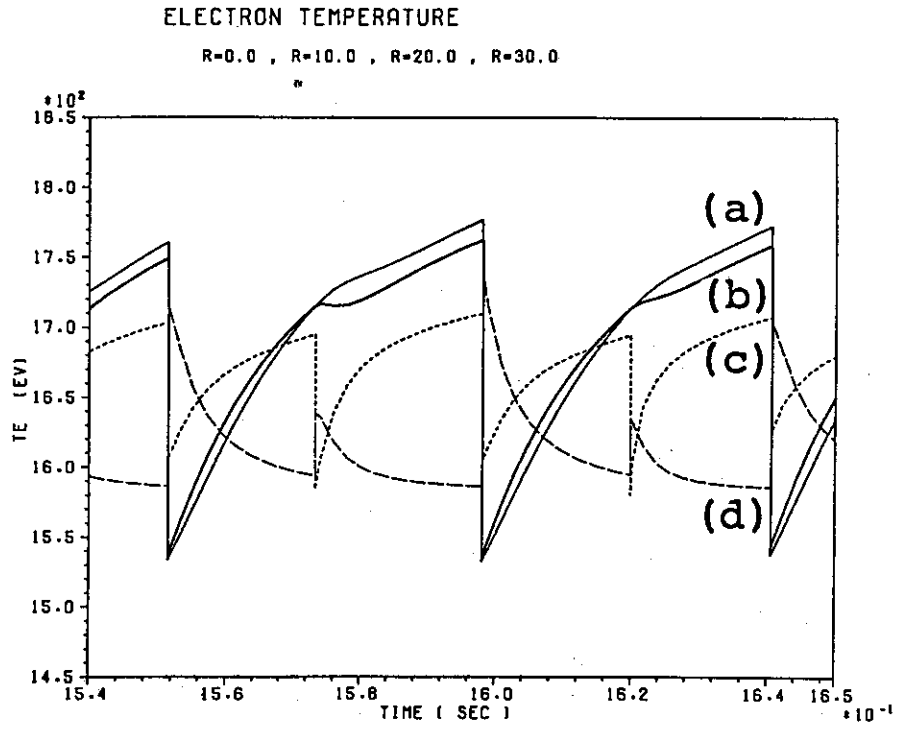

Fig. 12 Time evolution of electron temperature by numerical calculation at (a) r = 0 cm, (b) r = 10 cm, (c) r = 20 cm, (d) r = 30 cm in 2.0 MA hydrogen plasma. Double sawtooth oscillations with the period of 50 msec are observed.

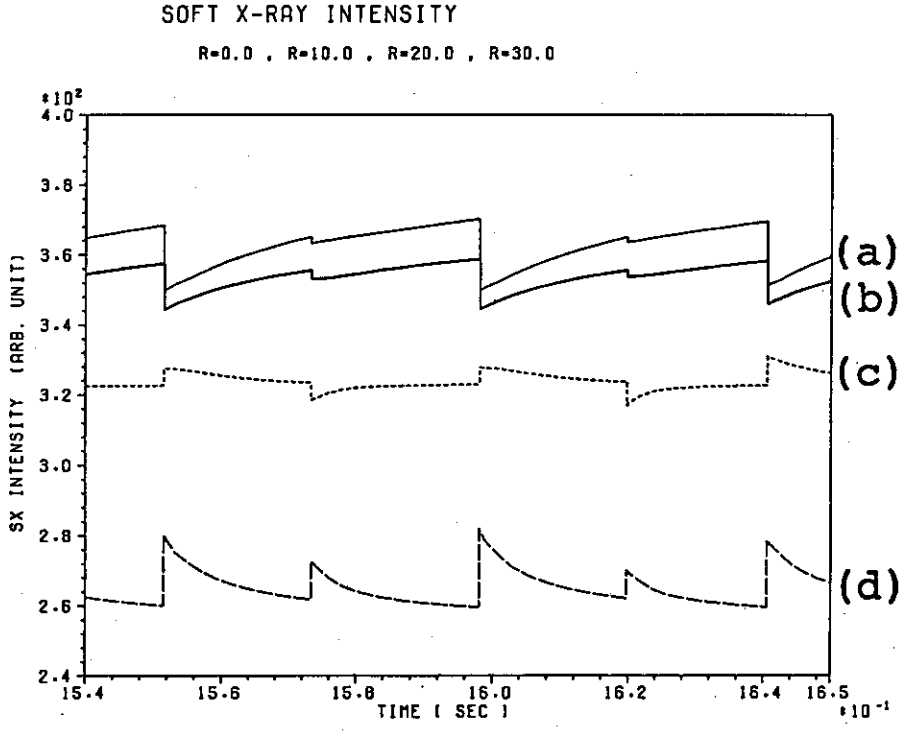

Fig. 13 Time evolution of soft X ray intensity by numerical calculation in 2.0 MA hydrogen plasma. The distance between plasma center and viewing chord is (a) r = 0 cm, (b) r = 10 cm, (c) r = 20 cm, (d) r = 30 cm respectively.

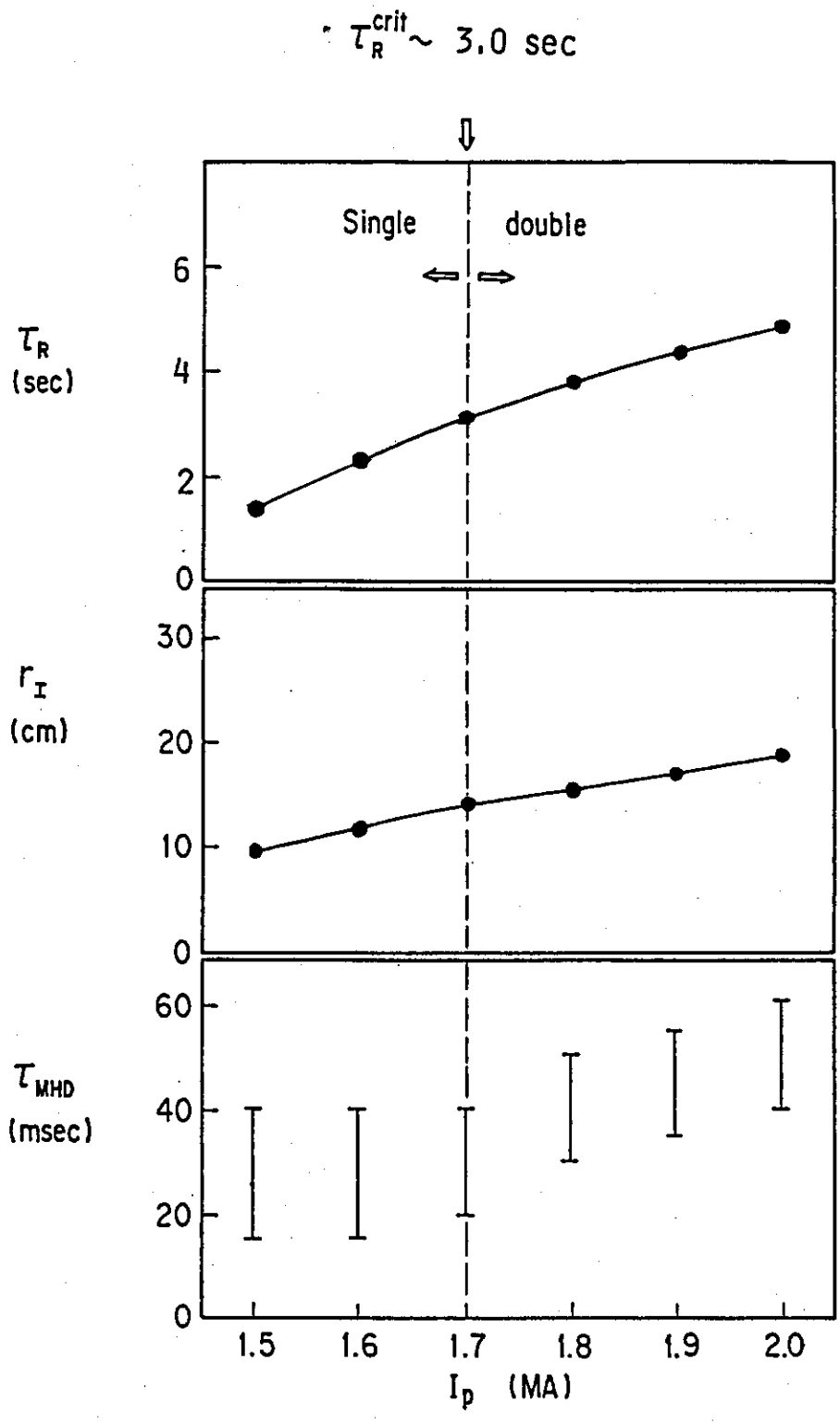

Fig. 14 Numerically calculated resistive skin time τ_R, inversion radius of soft X ray intensity r_I and period of sawtooth oscillations τ_{MHD} by various value of plasma current. Transition from single sawtooth oscillations to double sawtooth oscillations occurs at τ_R = 3.0 sec.

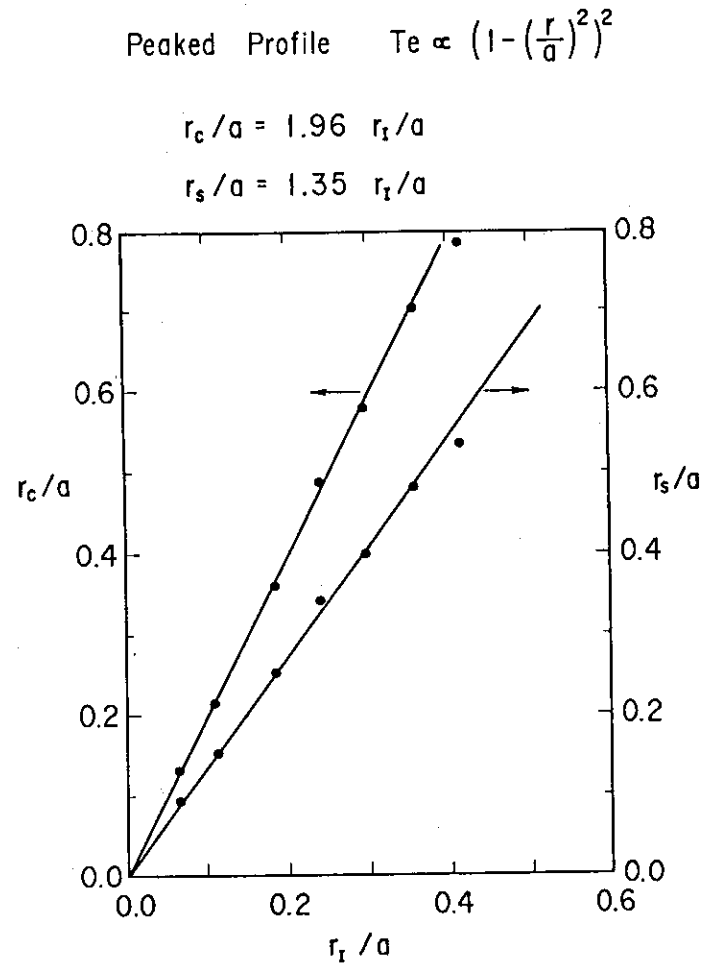

Fig. 15 Values of r_s/a and r_c/a are plotted by the function of r_I/a in the peaked temperature profile. Approximately, r_s/a = 1.35 r_I/a and r_c/a = 1.96 r_I/a.

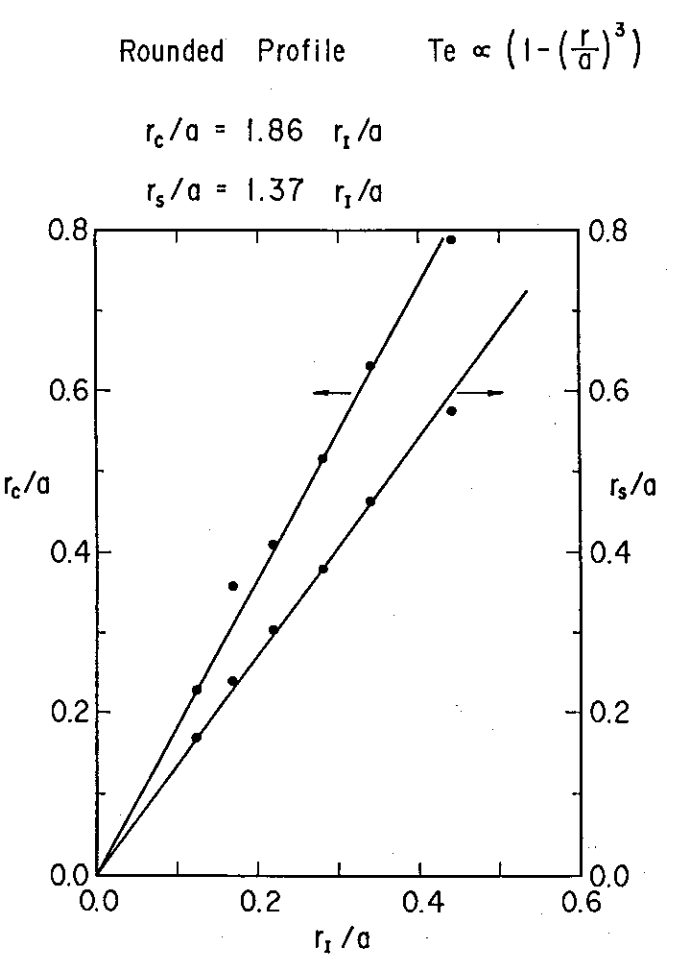

Fig. 16 Values of r_s/a and r_c/a are plotted by the function of r_I/a in the rounded temperature profile. Approximately, r_s/a = 1.37 r_I/a and r_c/a = 1.86 r_I/a

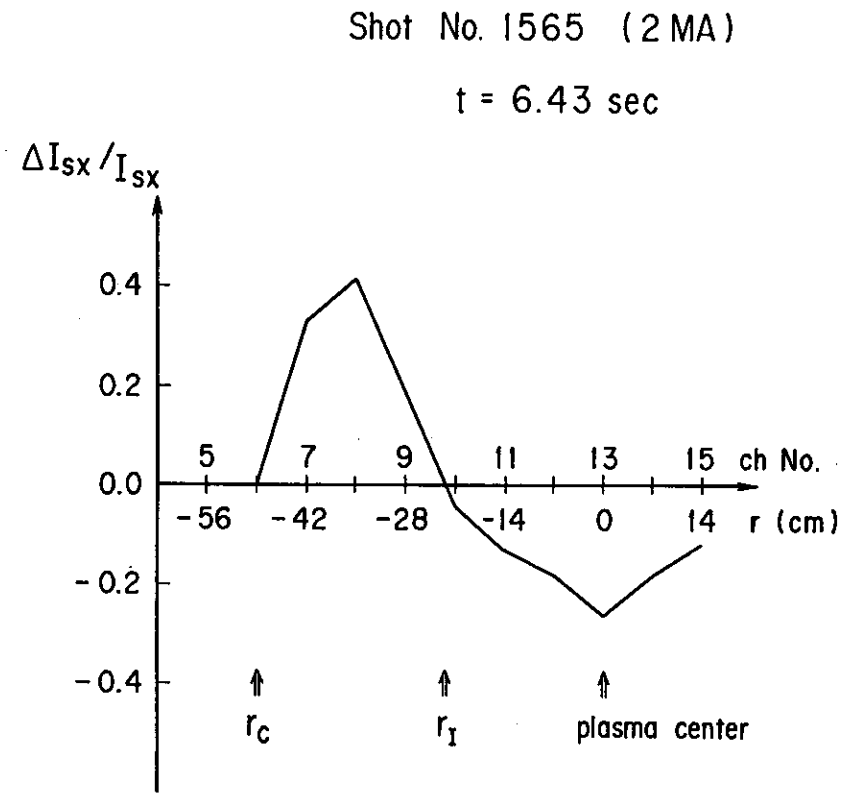

Fig. 17 Profile of change in soft X ray intensity $\Delta I_{SX}/I_{SX}$ at the different viewing chords at the minor disruption in 2.0 MA hydrogen plasma. Arrows indicate the positions of plasma center, r_I and r_c . Approximately $r_c = 2\ r_I$.

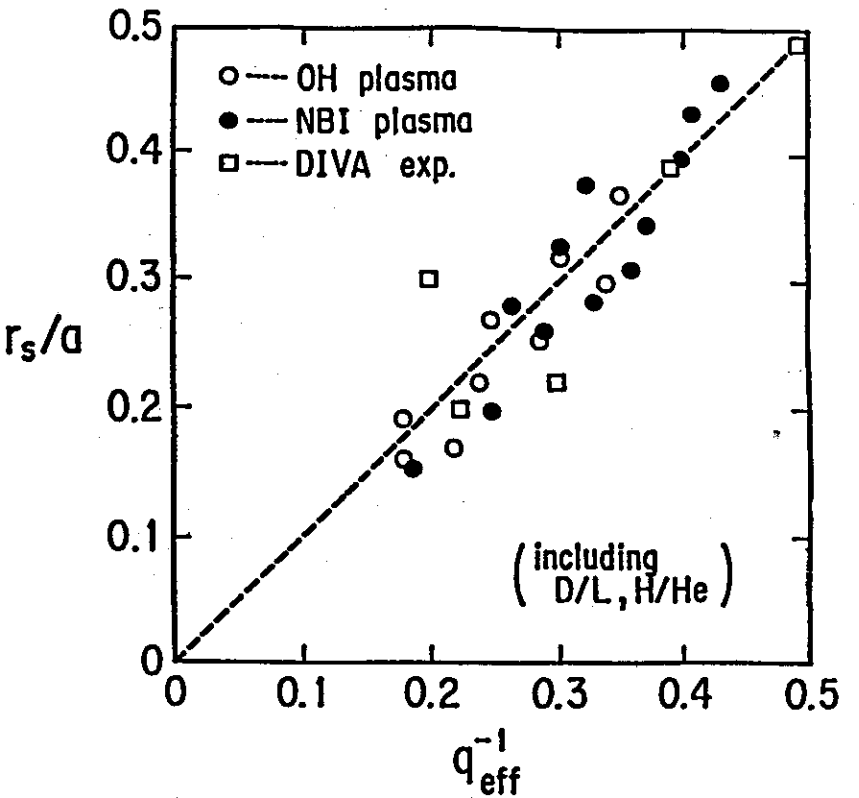

Fig. 18 Dependence of normalized q=1 resonant surface on q_{eff}^{-1}. Open circle indicates JT-60 OH plasma. Close circle indicates JT-60 NBI plasma. Open square indicates DIVA plasma. Approximately, $r_s/a = q_{eff}^{-1}$.